PCCP

Interaction between probe molecules and zeolites.

Part I:† Pair-wise addition scheme applied to the calculation of the interaction energy of CO and N_2 adsorbed in Na_4Ca_4A

A. V. Larin,[a] L. Leherte[b] and D. P. Vercauteren*[b]

[a] *Institute for Studies in Interface Sciences, Laboratoire de Physico-Chimie Informatique, Facultés Universitaires Notre Dame de la Paix, Rue de Bruxelles 61, B-5000 Namur, Belgium*
[b] *Laboratory of Molecular Beams, Department of Chemistry, Moscow State University, Vorob'evy Gory, Moscow, B-234, 119899 Russia*

Received 9th August 2001, Accepted 29th January 2002
First published as an Advance Article on the web 29th April 2002

An important problem when studying the interaction between a CO probe molecule and a Na_4Ca_4A type zeolite is the estimation of the central repulsive coefficients *versus* the internuclear distance of CO. In particular, this dependence cannot be estimated in the case of the unstable linear "framework oxygen–CO molecule" pair due to the electrostatic repulsive interaction. Hence, we discuss the application of two approximate forms of this dependence either allowing or disregarding the repulsive contribution in the interval wherein the vibrational CO probability distribution cannot be neglected. The consequences of these approximations are compared through calculation of the interaction energy and band shift of CO adsorbed inside Na_4Ca_4A. The CO spatial parameters (semi-axes) are estimated by fitting both the band shift, corresponding to two different positions of CO relative to the zeolite, and the interaction energy values to the experimental data obtained at small coverage.

I. Introduction

The choice of a probe molecule to characterize the acid strength of solid catalysts such as zeolitic frameworks is usually guided by the necessity of recording vibrational spectra of the probe located at Lewis and Brønsted centres.[1] CO is one of the few molecules whose use permits such a possibility at low coverage[1] and, hence, it has become one of the most popular molecular probes and its spectrum interpretations have stimulated the development of numerous theoretical models.[2–8]

Most of the approaches for the study of adsorbed CO are based on charged[9–13] (limited to a cation in the simplest cases)[9,13] or neutral[14–18] clusters, sometimes taking into account, but very often neglecting, the electrostatic field effects of the surrounding media. Avoiding the costly calculations of the CO vibrational frequency with *ab initio* quantum mechanical (QM) schemes, satisfactory interpretations of spectroscopic data for different CO positions relative to an oxide[16] or a zeolite[14] cluster were, for example, obtained within semi-empirical approaches, without even considering the electrostatic field effects.[14] The importance of electron correlation[19] as well as of the electrostatic effects was however clearly emphasized through studies performed with advanced QM approaches.[10–11,15,19,20] As a consequence of the crucial electrostatic contribution in zeolites, several models were developed considering merely the electrostatic influence of the adsorbent.[4,7–8,21]

The determination of the molecular positions inside an adsorbent should take into account all components of the interaction energy (IE), *e.g.*, electrostatic, inductive, dispersive, exchange-overlap, which all contribute to the vibrational band shift (BS) value.[22] The contributions to the IE may, for example, be evaluated through energy decomposition procedures like the constrained space orbital variation analysis.[10–11,17] Using this decomposition, it was shown that the back-donation charge transfer component could be of the same magnitude as the electrostatic IE only in the case of an exchangeable proton or transition metal ions (Cu^+) included in an oxide cluster.[11] Despite promising interpretations that could be deduced from *ab initio* QM calculations, other precise approaches such as embedded cluster[15] or QM/MM[18,20] clearly require further developments of model potentials between the interacting subsystems, especially with correct consideration of the long-range interactions with the part of the zeolite structure not included in the cluster subpart.

The importance of the repulsive interaction contributions for vibrational shift calculations was demonstrated more than thirty years ago by Friedmann and Kimel.[3] Therefore, BS calculations with pair-wise addition schemes require precise knowledge of the probe internuclear distance ρ dependence of all properties, *i.e.*, moments and polarizabilities of the probe, dispersive and repulsive coefficients of all "adsorbent atom–probe" pairs, which are necessary to describe the interacting system. The ρ dependence of the repulsive coefficients is usually determined from the equilibrium position condition of the adsorbed molecule relative to an ion or atom of the matrix[3] or adsorbent.[23–26]

When the pair-wise scheme is applied to the calculation of IE values for systems including highly-charged ions, the total IE between these highly-charged ions and a heteronuclear diatomic molecule can be repulsive. This is typically the case for the interaction considered in this paper, namely between a negative framework oxygen ion and CO.[26] The repulsion term (or the exchange-overlap IE) has a non-zero value. Neglecting this repulsion then generates an error in both the IE and BS values. An effective estimate of the repulsive coefficients' dependence on ρ is thus necessary for the CO case. This is exactly the problem we wish to discuss in the present paper.

† Fof part II see [ref. 58].

 DOI: 10.1039/b107243a

As soon as the most accurate calculation of the BS values is necessary, all terms of the IE should include dependences *versus* the internuclear C–O distance. Variations of the CO multipole moments and polarisabilities with the C–O distance in the gas state are well known and suggest the utilisation of a "molecule–atom" pair-wise addition scheme for the calculation of the total IE, even if the advantages of "atom–atom" representations have been demonstrated in many cases where only the IE is required. The "one-centre" model usually has a lower number of parameters to quantify than a two-centre model.

In Section II, we present the expressions for the IE components, the CO characteristics, the method for the BS calculation, and the models considered for the Na_4Ca_4A zeolite. We briefly compare different models of the internuclear potential of the CO molecule in the gas state in Section III.A, while the spatial CO model is presented in Section III.B. Then, we induce the approximate ρ dependences of the repulsive coefficients and show their influence on the calculated IE and BS values with different evaluation schemes (Section III.C). Calculation of the CO semi-axes from the IE and BS using two approximate ρ dependences is explained in Section III.D. For comparison of the calculated IE values, we also consider a simpler probe interacting with the same zeolite models, *i.e.*, N_2.

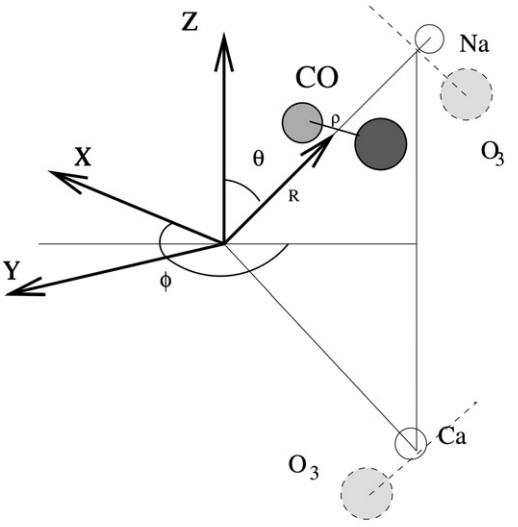

Fig. 1 Scheme of the coordinate system of CO inside the NaCaA zeolite cavity (CO position with O close to O_3).

II. Theory

II.A. Interaction energy calculation

The total IE, U_{tot} between the adsorbed CO and the zeolite framework can be evaluated as the sum of the electrostatic U_{elec}, inductive U_{ind}, dispersive U_{disp}, and repulsive U_{rep} interaction contributions. Charge transfer contributions are usually omitted in the total IE expressions, as well as for the BS, as their magnitudes are small compared to the electrostatic terms for CO interacting with an adsorbent without transition metal ions.[13] The electrostatic term can be expressed as:

$$U_{elec} = \sum_L U_{elec}^L \tag{1}$$

$$U_{elec}^L = \sum_i Q_L q_i P_L^0(\cos\theta_i) R_i^{-(L+1)} \tag{2}$$

where q_i is the charge of the framework ion i; R_i, the distance between the CO molecular centre of mass (COM) and ion i (Fig. 1); θ_i, the angle between the CO molecular axis (directed from the negatively charged C to the positively charged O atom) and the intermolecular axis (directed from ion i to the molecular COM); $P_L^0(\cos\theta_i)$, the associated Legendre polynomial; and Q_L, the central molecular moment of Lth order, for which we use the standard notation, namely, $Q_1 = \mu$, $Q_2 = \Theta$, $Q_3 = \Omega$, and $Q_4 = \Phi$.

Both theoretical[27] and experimental[28] dependences of the CO dipole moment on its internuclear distance ρ were used in this study (Table 1). They nearly coincide, but provide different estimations of the CO spatial models (see Section III.D). The dependences of the other moments, taken from the literature,[29–36] were approximated *via*:

$$Q_L(\rho) = \sum_{i=0}^{N} P_i(\rho - \rho_e)^i \tag{3}$$

where the equilibrium distance $\rho_e = 2.1322\ a_0$ for CO[33] and $2.076\ a_0$ for N_2,[29] and for which the coefficients P_i are given in Table 2.

The inductive IE has been determined using the following expression which includes terms proportional up to the second hyperpolarizability:

$$U_{ind} = -(1/2)(\alpha_\perp \cos^2\theta_F + \alpha_\parallel \sin^2\theta_F)F^2 - (1/6)\beta F^3 - (1/24)\gamma F^4 \tag{4}$$

where θ_F is the angle between the CO molecular axis and the electrostatic field vector at the molecular COM position; F, the electrostatic field value at the same position; and $\alpha_\perp$, $\alpha_\parallel$, β, γ, the perpendicular and parallel static polarizability components, and the averaged first and second hyperpolarizabilities, respectively. These values are presented in Table 1 using expansion (3) with $N = 4$.[27]

Table 1 Internuclear distance dependence $X(\rho) = \sum_{i=0}^{4} P_i(\rho - \rho_e)^i$ of the dipole moment μ, average polarizability α, polarizability anisotropy $\Delta\alpha$ (parallel $\alpha_\parallel$ and perpendicular $\alpha_\perp$ polarizabilities are expressed as $\alpha_\parallel = \alpha + 2\Delta\alpha/3$, $\alpha_\perp = \alpha - \Delta\alpha/3$, a_0^3), first β_{zzz}, and second γ_{xxxx} and γ_{zzzz} hyperpolarizability components (in $e^2\ a_0^3\ E_h^{-1}$ and $e^2\ a_0^4\ E_h^{-1}$, respectively, for CO ($\rho_e = 2.1322\ a_0$, $a_0 = 0.5292 \times 10^{-10}$ m) and N_2 ($\rho_e = 2.076\ a_0$)

Molecule	X	P_0	P_1	P_2	P_3	P_4
CO	μ^a	0.057	−0.6636	0.0008	0.1337	−0.0054
	μ^b	0.048	−0.6533	0.0304	0.148	−0.0440
	α	13.19	5.52	1.74	−0.35	−0.33
	$\Delta\alpha$	3.66	8.28	3.32	−0.24	−0.42
	$\beta_{zzz}{}^c$	30.0	−7.2	−8.3	−9.4	2.1
	$\gamma_{xxxx}{}^c$	1400	−47	1575	90	−483
	$\gamma_{zzzz}{}^c$	1860	1101	759	323	407
N_2	$\alpha_\perp$	10.126[d]	3.55[e]	0.26[e]	—	—
	$\alpha_\parallel$	14.774[d]	9.80[e]	1.76[e]	—	—

[a] Ref. 27. [b] Ref. 28. [c] Our approximation from ref. 27. [d] Ref. 29. [e] Our approximation from ref. 30.

Table 2 Internuclear distance dependences $Q_L(\rho) = \sum_{i=0}{}^{2} P_i\,(\rho - \rho_e)^i$ of the quadrupole Θ, octupole Ω, and hexadecapole Φ moments (in $ea_0{}^L$, $ea_0 = 8.478 \times 10^{-30}$ C m, $ea^2 = 4.486 \times 10^{-40}$ C m^2, $ea_0{}^3 = 2.374 \times 10^{-50}$ C m^3, $ea_0{}^4 = 1.256 \times 10^{-60}$ C m^4), for CO ($\rho_e = 2.1322\ a_0$, $a_0 = 0.5292 \times 10^{-10}$ m) and N_2 ($\rho_e = 2.076\ a_0$)

Molecule	Q_L	P_0	P_1	P_2	Ref.
CO	$\Theta^{a\,b}$	−2.92	0.91	0.83	35,36
	Ω	3.59	2.03	−0.43	35,36
	Φ	−9.10	−7.404	1.79	36
N_2	Θ^a	−2.22	1.14	−0.43	29,30
	Φ	−6.76	2.61	1.43	29,30

[a] $\Theta = 2\Theta_{zz}$. [b] For CO, P_0 values for $L = 2$–4 from ref. 36 and P_1 and P_2 from the fitting of CI calculations in ref. 33.

The dipole–dipole dispersive IE for each framework ion i has been considered through:

$$U_{\text{disp}} = -\sum_i C(\theta_i, \varphi) R_i^{-6} \tag{5}$$

wherein $C(\theta_i, \varphi)$ expresses the anisotropic dependence of the dipole–dipole dispersive interaction:

$$C(\theta_i, \varphi) = (3(C_{i\parallel} - C_{i\perp})\cos^2\theta_i + C_{i\parallel} + 5C_{i\perp})/6 \tag{6}$$

in which the van der Waals (vdW) dipole–dipole coefficient C_{ij} between the framework ion i and the adsorbed CO (or N_2) molecule in orientation j is estimated *via* the Kirkwood–Muller (KM) intercombination rule:

$$C_{ij} = 3/2\,\alpha_i\alpha_j/((\alpha_i/n_i)^{1/2} + (\alpha_j/n_{\text{AB}})^{1/2}) \tag{7}$$

where α_i and n_i are the static polarizability and number of electrons of the framework ion i, respectively, and α_j and n_{AB} are the static polarizability and number of electrons of the AB probe molecule (j corresponding to the parallel and perpendicular ion–molecule orientations without differentiation between i–AB and i–BA configurations), respectively. In eqn. (7), the number of electrons is $n_{\text{CO}} = n_{\text{N2}} = 14$, and $n_i = n_{oi} - q_i$, n_{oi} being the total number of electrons for the neutral atom. Eqn. (7) can be used in the KM case, if the diamagnetic susceptibility is expressed *via* α_i and n_i,[37] *e.g.*, in au: $\chi_i = \sqrt{n_i\alpha_i}/(4c^2)$, c being the velocity of light.

Higher order terms of the dispersive IE were omitted in this paper because the KM rule usually overestimates the vdW coefficients given by eqn. (7). Detailed discussions of the influence of the dipole–quadrupole dispersive interaction (where other intercombination rules are used) on the calculated total IE and BS values will be presented in a further paper.[38]

The repulsive IE has been expanded as an R^{-12} dependent contribution:

$$U_{\text{rep}} = \sum_i \{B_{i\perp}\sin^2\theta_i + (B_{i\text{–CO}} + (B_{i\text{–OC}} - B_{i\text{–CO}}) \times \sin^2(\theta_i/2))\cos^2\theta_i\} R_i^{-12} \tag{8}$$

the repulsive coefficients, $B_{i\text{–OC}}$, $B_{i\text{–CO}}$, and $B_{i\perp}$, being calculated at the equilibrium position for all "framework atom i–OC or CO" pairs with $\parallel$ or $\perp$ orientation, respectively, through derivatives $(U_k)' = (\mathrm{d}U_k/\mathrm{d}R_{ij})$ with respect to the intermolecular distance R_{ij} of all components for the total interaction energy U_{tot}:

$$B_{i\text{–OC}} = R_{ij}^{13}\left(\sum_k (U_k)'\right)\Big/ 12 \tag{9}$$

where R_{ij} is the sum of the vdW radii of the framework atom i and of the probe molecule within the j-orientation, *i.e.*, OC, CO $\parallel$, and CO $\perp$.

The electrostatic repulsive interaction could lead to a total repulsive interaction for the pair O_{zeol}–CO, which may even take place in the vibrational ground state of the CO molecule but it usually appears at distances $\rho < \rho_e$. In these cases, the repulsive coefficients $B_{\text{O–CO}}$ can be estimated either:

(a) from the derivative of the dispersive IE (eqn. (5)):

$$B^*_{\text{O–CO}} = (C_{\text{O}}/12)R_{\text{O}}^6 \tag{10}$$

where $C_{\text{O}} = 4C_{\text{O}\parallel} + 2C_{\text{O}\perp}$ for a parallel probe orientation, and $C_{\text{O}\parallel} + 5C_{\text{O}\perp}$ for the perpendicular one;

or (b) from eqn. (9), in which the derivatives $(U^1_{\text{elec}})'$ and $(U^3_{\text{elec}})'$ causing the repulsion are omitted.

The asterisk in both (a) and (b) estimations of the repulsive coefficients is used to distinguish them from the correct coefficient evaluated by eqn. (9). Case (b) is considered below only for illustration.

The angular dependence of the repulsive potential eqn. (8) was chosen to satisfy the requirement of the limiting value of the average repulsive coefficient B_{av} of a free rotating molecule:

$$\begin{aligned} B_{\text{av}} &= \int \mathrm{d}\theta_i \sin\theta_i \{B_{i\perp}\sin^2\theta_i + (B_{i\text{–CO}} + (B_{i\text{–OC}} - B_{i\text{–CO}}) \\ &\quad \times \sin^2(\theta_i/2))\cos^2\theta_i\} \Big/ \left(\int d\theta_i \sin\theta_i\right) \\ &= (4B_{i\perp} + B_{i\text{–OC}} + B_{i\text{–CO}})/6 \end{aligned} \tag{11}$$

II.B. Spatial CO model

In order to construct the spatial CO model that is required for the calculation of the repulsive coefficients, we propose the following procedure. Firstly, a sphere of vdW radius r_{m} is converted to an ellipsoid or a spherocylinder of the same volume. This requirement gives a third-order equation which allows us to find the semi-axes of both volumes:

$$r_\perp{}^3 + a\rho_e\Delta_\parallel^\perp r_\perp{}^2 - (r_{\text{m}}/2)^3 = 0 \tag{12}$$

where $\Delta_\parallel^\perp = (r_\parallel - r_\perp)/\rho_e$ is a dimensionless parameter, ρ_e being the CO equilibrium internuclear distance, and $a = 1$ or $3/2$ for the ellipsoid or spherocylinder type volume, respectively. Secondly, the sum of the radii of the C and O atoms ($r_{\text{C}} + r_{\text{O}}$) must be equal to the parallel diameter $2r_\parallel$ of the molecule. Three parameters $r_\perp$, r_{C}, and r_{O} thus determine the spatial representation of the molecule, and the isotropic vdW radius may be expressed for the ellipsoid case as:

$$r_{\text{m}} = 2[r_\perp{}^2(r_{\text{C}} + r_{\text{O}})/2]^{1/3} \tag{13}$$

II.C. Band shift calculation

The BS calculations were performed using two different approaches. Firstly, we applied a numerical procedure:[23–26]

$$\Delta\nu_{\nu-\nu'} = \frac{1}{hc}((E_\nu^{\text{ads}} - E_\nu^{\text{ads}}) - (E_{\nu'}^{\text{gas}} - E_{\nu'}^{\text{gas}})) \tag{14}$$

where the eigenvalues, E_ν^{ads} and E_ν^{gas}, are the solutions of the one-dimensional vibrational equation solved as implemented

in the LEVELS code:[39]

$$\left(-\frac{1}{2m}\frac{\mathrm{d}^2}{\mathrm{d}\rho^2}+V(\rho)-E_v\right)|v\rangle=0 \qquad (15)$$

where $E_v = E_v^{\mathrm{ads}}$ for $V(\rho) = V_0(\rho) + U_{\mathrm{tot}}(\rho)$ in the adsorbed state, or $E_v = E_v^{\mathrm{gas}}$ for $V(\rho) = V_0(\rho)$ in the gas state, $V_0(\rho)$ being the potential of the free probe molecule. Such BS estimation means that any coupling between the probe internuclear vibration and the zeolite modes is neglected. It can be justified by the relatively higher vibration frequency of the diatomic molecules as compared to the modes of the high temperature pre-treated cationic zeolite frameworks, *i.e.*, without hydroxy groups.

The BS contribution from the differences between the energy levels of a hindered rotator as in the case of CO can be estimated *a priori* as negligible. Small contributions to the total value $\Delta\nu$ may also come from the differences between the energy levels of the vibrations of the COM in the upper and lower states of the internuclear fundamental vibrational transition $|1\rangle \leftarrow |0\rangle$. These respective BS values $\Delta\nu_{\mathrm{R}}$ due to the COM vibration:

$$\Delta\nu_{\mathrm{R}} = \frac{1}{hc}\left(E_0^1 - E_0^0\right) \qquad (16)$$

were also obtained[25] through the numerical procedure implemented in the LEVELS code.[39] The COM motion was considered as non-interacting with the other motions:

$$\left(-\frac{1}{2M}\frac{\mathrm{d}^2}{\mathrm{d}R^2}+U^{\nu}(R)-E_{\nu_{\mathrm{R}}}^{\nu}\right)|\nu,\nu_{\mathrm{R}}\rangle=0 \qquad (17)$$

where M is the reduced mass of the total zeolite[25] and probe system, and v_{R} is the quantum number of the vibration of the probe COM.

II.D. The NaCaA zeolite model

The approximations applied to derive a reasonable zeolite model based on the IR spectrum of adsorbed hydrogen were presented earlier.[23–26] Three unknown parameters per ion type, *i.e.*, atomic charge, polarizability, and radii are necessary for calculation of the IE by empirical methods. The total number of unknown variables is thus $N = 3K$, K being the number of different ion types. For zeolite NaCaA, composed of Na, Ca, Al, Si, and O ions, $K = 5$. The number N may be decreased by constraining the charge dependences of the polarizabilities and radii.[40] These dependences are given in Table 3. Then the number of unknown variables corresponds to the $(N-1)$ charges.

Atomic charges can be expressed through a unique ionicity value q_0 (in e) as:

$$\begin{aligned} q_0 &= (1/3)[q(\mathrm{Ca}) + q(\mathrm{Na})] + q(\mathrm{Si}) + q(\mathrm{Al}) \\ &= |\, q(\mathrm{O}_1) + q(\mathrm{O}_2) + 2q(\mathrm{O}_3)\,| \end{aligned} \qquad (18)$$

where the indices are related to the three different oxygen types present in zeolite A. The right part is equal to $4|q(\mathrm{O})|$, if all O types are equivalent. Allowing that the ratio $q(\mathrm{Al})/q(\mathrm{Si})$ does not influence the total IE, this ratio can be considered as constant. For H_2 adsorbed in zeolite NaCaA,[25] we were thus handling a problem of three variables, q_0, $q(\mathrm{Ca})$, and $q(\mathrm{Na})$, and two experimental values, the BS and band splitting. Two variables, q_0 (which can differ from q_0 for zeolite NaA) and $q(\mathrm{Na})$, were sought from the fitting of the BS and of the band splitting for H_2 adsorbed in zeolite NaA. Knowing $q(\mathrm{Na})$, the other two variables, $q(\mathrm{Ca})$ and q_0, may be obtained from the respective H_2 spectra in NaCaA.

All framework ions[43,44] of seven α-cages of the zeolite were considered to estimate the total IE between the zeolite and the probe.[45] However, because the rotational contribution to the band splitting could not be estimated precisely because of the sophisticated H_2 behaviour near the Ca ion, we considered a series of different fitted models which provided a good agreement with the experimental BS for H_2.[38] We fixed the values $f_1 = q(\mathrm{O}_1)/q(\mathrm{O}_2)$ and $f_2 = q(\mathrm{O}_3)/q(\mathrm{O}_2)$ in accordance with semi-empirical estimations $f_1 < 1$ and $f_2 > 1$.[46,47] In this way, we obtained two different models (A and B in Table 4). The higher ionicity of the models as compared to NaA may be explained as a result of a stronger coordination of the Ca by the framework oxygens. Hence, the two models of NaCaA presented correspond to lower Na charge values (0.5 and 0.6 e) than the NaA case (0.7 e). A charge ratio of $q(\mathrm{Al})/q(\mathrm{Si}) = 0.75$, slightly higher than for NaA (0.575), was taken

Table 3 Polarizability α (a_0^3) and radius r (a_0) functions expressed as linear $X(q) = X(0) - Aq$ or exponential $X(q) = X(0)\exp(G-q)/A)$ functions with charge q for Na, Ca, Si, Al, O (see ref. 23 for detailed explanation)

Ion	$X(q)$	q-Dependence	$X(0)$	A
Na	α	Linear	29.78	27.98
	r	Linear	2.91	1.058
Ca	α	Linear	40.0[a]	18.414[b]
	r	Linear	3.29[a]	0.7086[c]
O	α	Linear	7.55	9.38
	r	Linear	2.87	0.548
Si	α	Exponential[d]	0.013	19.13/12.39
	r	Linear	2.23	0.554
Al	α	Exponential[d]	0.109	19.40/10.70
	r	Linear	2.10	0.383

[a] Ref. 41. [b] Estimated A value considering $\alpha(\mathrm{Ca}^{+2}) = 3.178\ a_0^3$ from ref. 42. [c] Estimated A value considering $r(\mathrm{Ca}^{+2}) = 1.871\ a_0$ from ref. 42. [d] In the last column, A/G values coming from ref. 40 are presented instead of A.

Table 4 The two zeolite NaCaA models obtained by fitting ($\pm 1.6\ \mathrm{cm}^{-1}$) of the adsorbed H_2 band shift value to the experimental one ($-68.7 \pm 1.0\ \mathrm{cm}^{-1}$)[48] for a ratio $q(\mathrm{Al})/q(\mathrm{Si}) = 0.75$;[38] charges are in e

Model	q_0	q(Na)	q(Ca)	f_1	f_2	$q(\mathrm{O}_1)$	$q(\mathrm{O}_2)$	$q(\mathrm{O}_3)$
A	5.6	0.5	1.2	0.6	1.6	−0.7	−1.17	−1.87
B	7.5	0.6	0.9	0.9	1.05	−1.69	−1.88	−1.97

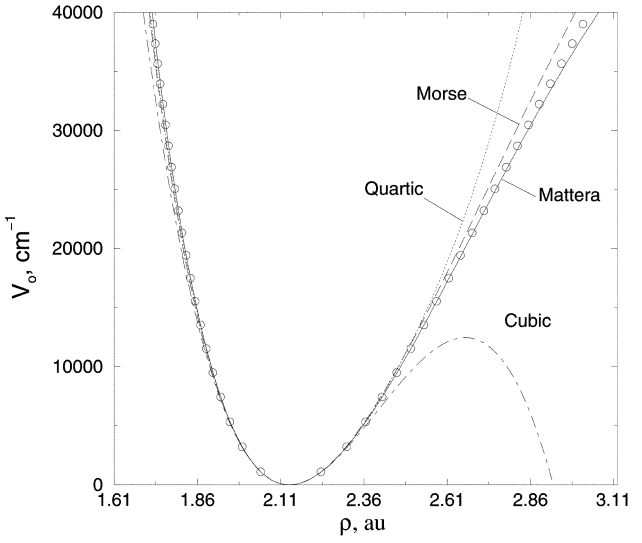

Fig. 2 Variation of the CO gas potential $V_0(\rho)$ with respect to its internuclear distance ρ considering various approximations (parameters from ref. 49 and 50). Rydberg–Klein–Rees potential points are shown as circles.[49]

Table 5 Influence of the CO gas potential $V_0(\rho)$ model on the numerical calculation (eqn. (14)) of the band shift values (in cm^{-1}) for CO positioned as Ca–CO ($\Delta\nu_C$) and Ca–OC ($\Delta\nu_O$) inside NaCaA considering model A presented in Table 4

Potential model	$\Delta\nu_C$	$\Delta\nu_O$
Mattera[49]	40.4	−29.8
Improved Morse[50]	40.6	−23.3
Morse[50]	38.2	−29.6
Quartic[50]	40.2	−28.1
Experimental[51]	40	−29

for NaCaA to avoid $q(\mathrm{Si}) > 4$, but this difference does not actually influence the resulting total IE.

III. Results and discussion

III.A. Vibrational energy levels calculation

First, we tested different types of CO potential curve approximation $V_0(\rho)$ (Fig. 2). We found that the quartic potential which is not appropriate for the estimation of the upper vibrational states leads to slightly better BS than both variants of the Morse potential (Table 5). In contrast to the H_2 case,[52] the differences between the BS values calculated with the different gas potential representations are rather negligible. Owing to the lower vibrational frequency of CO, all lowest levels are equally well described in the bottom of all approximated curves $V_0(\rho)$ (Fig. 2), including the cubic approximation.[53] The Mattera approximation[49] of the Rydberg–Klein–Rees potential was used below for the numerical estimation of the BS values.

In order to calculate satisfactory $V_0(\rho)$ and $U_{tot}(\rho)$ functions, we chose a grid of 100 equidistant points spaced by 0.0132 a_0 starting at 1.55 a_0. The expansion of the grid interval or decrease of the step shifts the BS by less than 0.2 cm^{-1}.

III.B. Interaction energy calculation and CO favoured sites

Three examples of the total IE variation with respect to the radial coordinate R are given in Fig. 3(a)–(c) for three different molecular positions presented in the coordinate system of the

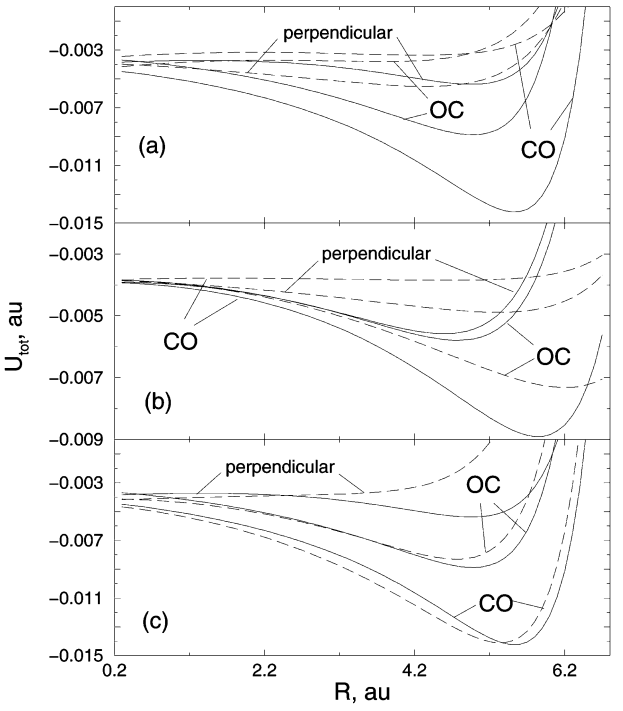

Fig. 3 Variation of the total interaction energy with respect to the radial coordinate R for different CO molecular positions inside the NaCaA zeolite (''CO'' corresponds to the C-term directed to the zeolite wall; ''OC'', to the O-term; ''perpendicular'', to the CO axis perpendicular to the respective symmetry axis): (a) Model B: Ca-ion direction ($\varphi = 1.75\pi$, $\theta = 0.304\pi$) (solid line), Na-ion direction ($\varphi = 1.75\pi$, $\theta = 0.696\pi$) (dashed line); (b) Model B: ''C_2''-axis direction ($\varphi = 1.5\pi$, $\theta = 0.25\pi$) (solid line), ''C_4''-axis direction ($\varphi = 1.5\pi$, $\theta = 0.5\pi$) (dashed line). (c) Ca-ion direction ($\varphi = 1.75\pi$, $\theta = 0.304\pi$): model B (solid line); model A (dashed line).

cavity (Fig. 1). In Fig. 3(c), we compare the variation of the total IE for the same three CO positions pointing along the same direction within the zeolite cage for both A and B models. The preferential location of CO was sought along the threefold axis with the C-term (negative charge) pointing closest to the Ca ion ($U_{tot} = -14.1 \times 10^{-3}\ E_h$, $R = 5.7\ a_0$), itself closest to O_3 included in the 6- and 4-membered rings of the framework (Fig. 3(c)). The intermolecular ''O_i–COM of CO'' distance at the preferential location increases according to the sequence $O_3 < O_2 < O_1$, in the same order as the distance ''O_i–Ca (or Na)''. As a result of the lower coordination by the Ca (or Na) cation, the absolute value of the framework O charge decreases in this same order $|q(O_3)| > |q(O_2)| > |q(O_1)|$[46,47] (Table 4). An example of the IE contributions is shown in Fig. 4 where the dispersive and electrostatic quadrupole terms dominate throughout all the attractive IE terms.

III.C. Influence of the approximation on the repulsive coefficients on the calculated interaction energy

In order to avoid an important error due to neglect of the repulsive interaction with any of the framework oxygen ions, one should propose an approximation of the repulsive coefficients for any O_i–CO configuration. Therefore, we compared the dependences of the repulsive coefficients $B^*_{O\text{–}CO}(\rho)$ obtained *via* eqn. (9) neglecting several derivatives of the IE components leading to the total repulsion with the coefficients $B_{O\text{–}CO}(\rho)$ calculated with all the derivatives of the IE (Fig. 5(a) and (b)). The dependences $B^*_{O\text{–}OC}(\rho)$ were applied for $\rho < \rho_{int}$ (at its left), where the condition $B^*_{O\text{–}OC}(\rho_{int}) = B_{O\text{–}CO}(\rho_{int})$ is satisfied. However, within the considered ρ range, $B^*_{O\text{–}OC}(\rho)$ dependences have essentially another slope as compared to

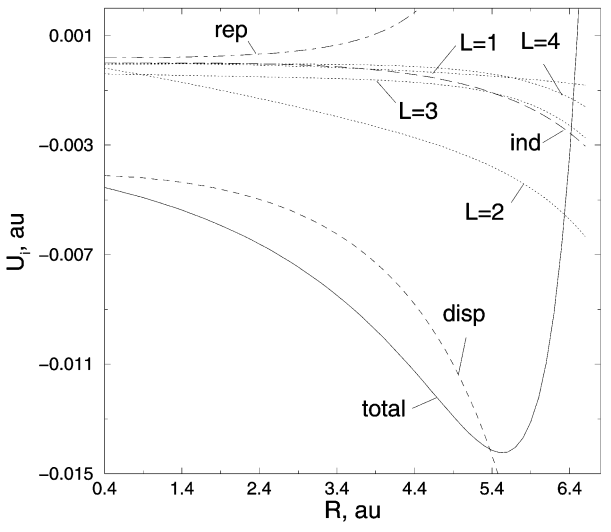

Fig. 4 Variation of the interaction energy components between CO and the NaCaA zeolite along the Ca-ion direction considering the zeolite model A: $U_{elec}{}^{L}$ (dotted lines with the L-order of the molecular multipole); U_{disp} (dashed line); U_{ind} (long-dashed line); U_{rep} (dot-dashed line); U_{tot} (solid line). The CO molecular model corresponds to that given in the first line of Table 7.

the repulsive coefficient calculated with eqn. (9), *i.e.*, the solid line for $\rho > \rho_{int}$ in Fig. 5. As a result, all BS values estimated by neglecting some of the derivatives of the IE in eqn. (9) are not correct. These variants of the $B_{O\text{–}CO}(\rho)$ approximation will thus not be considered any further.

One should note that the behaviour of $B_{O\text{–}CO}(\rho)$ (eqn. (9)) follows exactly the behaviour of the CO dipole moment with

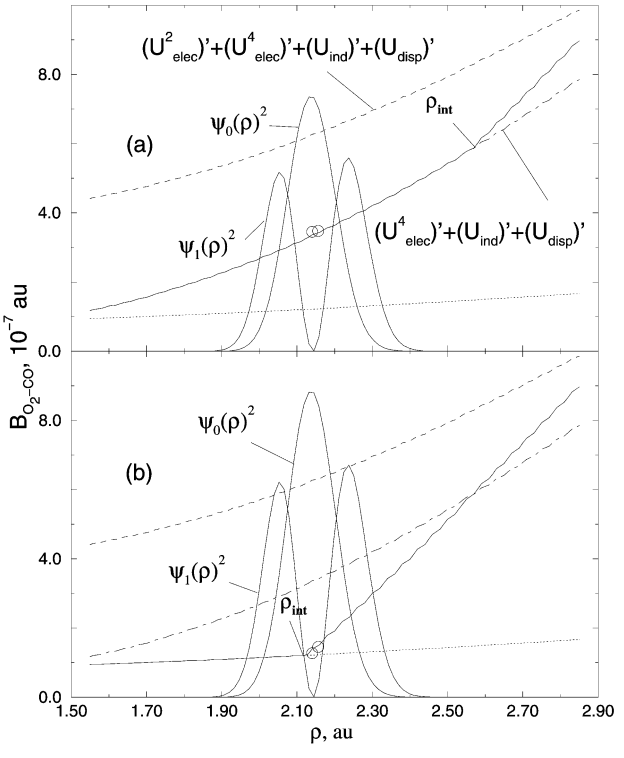

Fig. 5 Variation of the $B^{*}{}_{O_2\text{–}CO}$ repulsive coefficients *versus* the CO internuclear distance ρ for CO interacting with the NaCaA zeolite calculated using: (a) eqn. (9) with part of the derivatives (dashed and dot-dashed lines) or (b) eqn. (10) (dotted line). $B_{O_2\text{–}CO}(\rho)$ values obtained using eqn. (9) and all IE derivatives for $\rho > \rho_{int}$ (solid line). $B_{O2\text{–}CO}(\rho_v)$ ($v = 0$, 1) values are shown by circles for the $B_{O_2\text{—}CO}(\rho)$ dependence resulting from the combination of eqn. (9) and (10).

its internuclear distance ρ (solid line in Fig. 5(b)). The moment changes its sign at larger $\rho > \rho_0$ values, which corresponds to the inversion of the C and O charges and should lead to a stable O_{zeol}–CO configuration at higher vibrational states of CO. So, the solution that is proposed here is to extend the behaviour of the repulsive coefficient to shorter ρ values in the area where the vibrational CO probability distribution cannot be neglected.

We tried to replace the repulsive coefficient dependence within the remaining part of the ρ interval by a function $B^{*}_{O\text{—}CO}(\rho)$ (eqn. (10)) obtained from the derivative of the dispersive interaction component only (solid lines for $\rho < \rho_{int}$ in Fig. 5(b)). This evaluation led to the positioning of the intersection point ρ_{int} within the area of non-zero vibrational probability distribution (Fig. 5(b)). As a result, the repulsive coefficient $B_{O\text{–}CO}(\rho)$ dependence obtained *via* the summation over all derivatives remains valid for a larger ρ interval than the other "partial" variants of functions $B^{*}_{O\text{—}OC}(\rho)$ (Fig. 5(a)). Hence, the BS estimation should be closer to the value obtained using eqn. (9) considering all IE derivatives.

A correct comparison between the behaviour of the functions $B_{O\text{–}CO}(\rho)$ (eqn. (9)) and $B^{*}_{O\text{—}CO}(\rho)$ (eqn. (10)) for any internuclear CO distance requires the exact form of $B_{O\text{–}CO}(\rho)$, which should be calculated *ab initio* for any framework O atom stabilized by the lattice. The replacement by estimation (10) is however in agreement with the assumption of non-zero repulsion between CO and all ions of the zeolite. This assumption is not valid when neglecting part of the repulsive interactions for $\rho < \rho^{*}$:

$$B_{O\text{–}CO}(\rho) = 0, \quad \text{if} \sum_i U_i'(\rho) < 0 \tag{19}$$

The error of such neglect on the total IE is less than 3–5%, but the calculated BS is still of the same order of magnitude and thus the error should be taken into account. Evidently, the error on the BS is negligible for the Ca–OC configuration because the influence of the repulsive O_i–CO interactions is less important.

The result of both approaches, *i.e.*, either allowing or disregarding the repulsive interactions, is presented in Table 6 for the two zeolite models; a larger difference in the BS, 53.1 and 38.2 cm^{-1}, is observed for model B which presents a smaller difference between the O charges as compared to model A (Table 5). This larger difference between the estimations obtained *via* eqn. (10) and (19) for model B is the consequence of a nearly simultaneous cancellation of all repulsive coefficients (*i.e.*, with all O_3, O_2, and O_1 ions) due to their very similar radii and polarizabilities determined by their charges (Table 4). However, the difference between the resulting spatial CO parameters fitted *via* either eqn. (10) or (19), and with the B zeolite model should not be too large. This could be confirmed by allowing an analogous minor shift of 0.04 Å for the vdW radius r_m of CO fitted with the A model either *via* eqn. (10), or eqn. (19) (Table 7).

At high coverage, the CO probe could evidently be located at another site where the influence of the closest O_1 and O_2

Table 6 Influence of the chosen approximation of the repulsive coefficients expressed by eqns. (10) and (19) for CO (spatial model in the third line of Table 7) interacting with the NaCaA zeolite on the calculated band shift values (cm^{-1}) obtained *via* the numerical solution (eqn. (14)).

Model	Approximation	$\Delta\nu$
A	Eqn. (10)	48.1
	Eqn. (19)	41.1
B	Eqn. (10)	53.1
	Eqn. (19)	38.2

Table 7 CO spatial parameters (Å) obtained by fitting (± 1.3 cm^{-1}) the calculated band shift values and interaction energy ($-13.8 \pm 0.2 \times 10^{-3}$ E_h) for CO interacting with NaCaA to the experimental data with different CO dipole moment (μ) dependences with its internuclear distance

q_0/e	CO model	r_C	r_O	$r_\perp$	μ-dependence	r_m[b]
5.6	A[a]	2.09	2.25	2.09	Ref. 28	4.28
	B	2.03	2.2	2.25	Ref. 27	4.32
7.5	C	1.99	2.16	2.29	Ref. 28	4.29
	D	1.97	2.16	2.32	Ref. 27	4.29
Experimental						4.22, 4.099[c]

[a] With eqn. (10) for this model and eqn. (19) for other cases. [b] vdW radius r_m obtained *via* eqn. (13). [c] Ref. 54, average values from measurements of viscosity and cross-section of molecular beam scattering.

ions could be more important. Such a case was found for CO with the O-term directed towards the zeolite wall (with model A) along the C_2-axis of a cube whose corners are occupied by the Ca and Na cations ($\varphi = 1.5\pi$, $\theta = 0.25\pi$; the energy for this axis in zeolite model B being given by solid lines in Fig. 3(b)). The minimum IE value with respect to the radial coordinate of the COM of CO is equal to -8.52×10^{-3} E_h at $R = 5.75$ a_0 (3.04 Å) if approximation (10) is applied, and to -8.93×10^{-3} E_h at $R = 5.85$ a_0 with eqn. (19). So, a definite choice of the CO most stable location along the C_2-axis is ambiguous. This difference in the calculated probe locations suggests that one should be cautious while applying approximation (19) at the sites with close O atoms. Reasonable values of the IE and BS could be obtained by a combination of eqns. (10) and (19). A correct solution can be tested provided that eqns. (10) and (19) lead to close IE values and to the lower and upper BS, respectively, *via* the numerical solution (eqn. (14)).

III.D. Calculation of the CO molecular semi-axes

Both Ca–CO and Ca–OC orientations in the zeolite are important for the interpretation of the BS values at low coverage. Two bands were tentatively assigned[51] as corresponding to two opposite positions of CO relative to the Ca. The Ca–CO orientation is the favoured one for all NaCaA models studied in this work. The existence of a stable minimum along the threefold axis for the opposite Ca–OC orientation was obtained with respect to all five required coordinates of the CO molecule, *i.e.*, two rotational angles of the molecular axis and three spherical coordinates (R, θ, ϕ) of the molecular COM within the zeolite cage (Fig. 1). In so far as the NaCaA model has already been fitted,[38] it is possible to estimate the molecular semi-axis values, r_C, r_O, and $r_\perp$, which could be used for the analysis of any CO spectra recorded inside other zeolite frameworks. Two experimental BS values[51] are not enough to calculate the three semi-axes so we added the experimental heat of CO adsorption.[55] Because the BS obtained from the application of eqns. (10) and (19) correspond to the upper and lower BS estimations for the Ca–CO orientation, a comparison of the spatial molecular parameters determined using both approximations is needed.

For the two zeolite models given in Table 4, we fitted the BS corresponding to the two opposite orientations of CO relative to the Ca ion[51] and the differential heat of adsorption[55] to the experimental data by varying the molecular semi-axes r_C, r_O, and $r_\perp$ (Table 7). The consideration of the vibration of the COM *via* the numerical method (eqn. (16)) is not important in the cases of the BS of CO and N_2 (less than 0.5 cm^{-1}). All molecular models correspond to higher IE for the Ca–CO position in accordance with the experimental assignment.[51] All spatial models are close to each other and all overestimate slightly the known vdW radius r_m. The overestimated $r_\perp$ semi-axis deserves more attention due to an evident contradiction with the conventional CO models.

The reason for the overestimated $r_\perp$ semi-axis, *i.e.*, $r_\perp > (r_C + r_O)/2$, may be understood by analysis of the IE values for H_2 and N_2 adsorbed inside the NaCaA framework. The IE for o-H_2/p-H_2 ($-3.41/-3.55 \times 10^{-3}$ E_h from ref. 55) and N_2 (-12.24×10^{-3} E_h) calculated with, for example, the A model of NaCaA, overestimate the experimental heat of adsorption values (-2.7×10^{-3} E_h from ref. 56 and -2.95×10^{-3} E_h from ref. 55 for H_2, -8.3×10^{-3} from ref. 57 and -11.0×10^{-3} E_h[55] for N_2). This may be explained by the fact that the rotational contribution to the total BS was neglected for H_2 while fitting the zeolite models.[38] The molecular H_2 rotational model used for the description of the adsorption on Ca in NaCaA does not allow a quantitative description of the experimental splitting of the vibrational band for H_2[38] and as a result, the rotational BS contribution was not added to the total BS. Its inclusion should lead to a decrease in the total IE.[25] The calculated BS of N_2 in NaCaA, 3.9 and 5.2 cm^{-1} for models A and B, respectively, compared to the experimental value of 10 cm^{-1},[51] also demonstrates the overestimation of the dispersive and inductive components leading to enhanced negative contributions to the total BS.

If both zeolite models fitted without the rotational BS contribution lead to overestimated IE values for H_2 and N_2, we should obtain the same effect for CO. Then, by fitting the CO interaction with the zeolite framework by varying the semi-axis values, we should compensate for this increased interaction appearing from the distorted zeolite parameters by an overestimation of the molecular sizes. This may explain the overestimated values of the semi-axis $r_\perp$. However, this CO model (first line of Table 7) allows us to describe the BS of CO adsorbed in both NaY and NaRbY zeolites.[58] This fact allows us to confirm the transferability of the CO molecular sizes obtained herein to other zeolites.

IV. Conclusions

In this paper, we particularly studied the case of the unstable linear geometry of the CO molecule interacting with negative O ions stabilized by a lattice, which has already been remarked upon in the literature.[9] We discussed this situation for CO within the NaCaA zeolite. The electrostatic interaction components are the reason for the total repulsive IE between the linearly oriented CO and the negative O ion. Consequently, one cannot estimate the CO internuclear distance ρ dependence of the central repulsive coefficients or the repulsive interaction component of the IE and of the BS corresponding to the interaction between CO and the zeolite framework. The approximations proposed above for the repulsive coefficients are related to the behaviour of the CO dipole moment with its internuclear distance ρ. The moment changes its sign at larger $\rho > \rho_0$ values, which corresponds to the inversion of the C and O charges and should lead to a stable O_{zeol}–CO configuration at higher vibrational states of CO. Thus, it was proposed to extrapolate the behaviour of the repulsive coefficient to shorter ρ values to solve this problem. Within the remaining part of the ρ interval wherein this extrapolation is not available, two variants for the estimation of the repulsive coefficients dependence on ρ were compared: (a) neglecting this repulsion term between CO and the respective framework oxygens and (b) replacing the dependence on ρ of the repulsive coefficient by the variation with ρ of the dispersive IE contribution. We recommend the simultaneous application of the two approaches to control both the resulting IE and BS values for analogous systems.

A simultaneous fitting of both the IE and BS values to the available experimental data at low CO coverage within

Na_4Ca_4A allows us to obtain a reasonable estimation of the spatial size parameters of the CO molecule also using the approximations for the repulsive coefficients. The fitted spatial size parameters have been used recently[58] to describe the BS of CO adsorbed in both NaY and NaRbY zeolites. Quantitative coincidence achieved with this model for both the Na–CO and Rb–CO geometries within the Y zeolites confirms the transferability of the spatial CO model to other zeolite systems.

Further developments should be related to the calculation of the IE in terms of more precise models of the distributed multipole moments (MM)[59] of both the adsorbent and adsorbate. Therefore, we have already suggested the estimation of the Mulliken charges of all zeolite atoms through *ab initio* computations with advanced basis set levels[60–64] using the CRYSTAL code[65] of some zeolites with a relatively small number of atoms (or atomic orbitals) per unit cell (UC). Then, we found how to approximate the higher order MM by simple analytical functions with respect to the internal coordinates and the charges of each different crystallographic type of atom.[66] The advantage of this strategy is that these functions could be applied to other zeolites with a higher number of atomic orbitals per UC.

Acknowledgement

The authors wish to thank the FUNDP for the use of the Namur Scientific Computing Facility (SCF) Centre, a common project between the FNRS, IBM-Belgium, and FUNDP as well as Accelrys for the use of their data in the framework of the "Catalysis 2000" consortium. They are grateful for the partial support of the Interuniversity Research Program on Quantum Size Effects in Nanostructured Materials (PAI/IUAP 5/01) initiated by the Belgian Government. All the authors thank Dr F. Jousse for useful collaboration and Dr A. L. Tchougreeff for fruitful discussions.

References

1 J. A. Lercher, C. Gründling and G. Eder-Mirth, *Catal. Today*, 1996, **27**, 353.
2 R. M. Hammaker, S. A. Francis and R. P. Eischens, *Spectrochim. Acta*, 1965, **21**, 1295.
3 H. Friedmann and S. Kimel, *J. Chem. Phys.*, 1965, **43**, 3925.
4 N. S. Hush and M. L. Williams, *J. Mol. Spectrosc.*, 1974, **50**, 349.
5 B. N. J. Persson and R. Ryberg, *Phys. Rev.B*, 1981, **24**, 6954.
6 D. Weick and K. Kambe, *Surf. Sci.*, 1985, **152/153**, 346.
7 D. M. Bishop, *J. Chem. Phys.*, 1993, **98**, 3179.
8 C. Lamberti, S. Bordiga, F. Geobaldo, A. Zecchina and C. Otero Areán, *J. Chem. Phys.*, 1995, **103**, 3158.
9 (*a*) E. A. Colbourn and W. C. Mackrodt, *Surf. Sci.*, 1982, **117**, 571; (*b*) E. A. Colbourn and W. C. Mackrodt, *Surf. Sci.*, 1984, **143**, 391.
10 J. A. Mejias, A. M. Marquez, J. F. Sanz, M. Fernandez-Garcia, J. M. Ricart, C. Sousa and F. Illas, *Surf. Sci.*, 1995, **327**, 59.
11 M. Fernandez-Garcia, J. C. Conesa and F. Illas, *Surf. Sci.*, 1996, **349**, 207.
12 P. Reinhardt, M. Causà, C. M. Marian and B. A. Heß, *Phys. Rev. B*, 1996, **54**, 14 812.
13 A. M. Ferrari, P. Ugliengo and E. Garrone, *J. Chem. Phys.*, 1996, **105**, 4129.
14 S. Beran, *J. Phys. Chem.*, 1983, **87**, 55.
15 M. Causà, R. Dovesi and F. Ricca, *Surf. Sci.*, 1993, **280**, 1.
16 K. Jug and G. Geudtner, *J. Chem. Phys.*, 1996, **105**, 5285.
17 K. M. Neyman, V. A. Nasluzov and G. M. Zhidomirov, *Catal. Lett.*, 1996, **40**, 183.
18 M. Brändle and J. Sauer, *J. Mol. Catal. A*, 1997, **119**, 19.
19 F. Illas, G. Pacchioni, A. Pelmenschikov, L. G. M. Pettersson, R. Dovesi, C. Pisani, K. M. Neyman and N. Rösch, *Chem. Phys. Lett.*, 1999, **306**, 202.
20 J. Sauer, P. Ugliengo, E. Garrone and V. R. Saunders, *Chem. Rev.*, 1994, **94**, 2095.
21 D. K. Lambert, G. P. M. Poppe and C. M. J. Wijers, *J. Chem. Phys.*, 1995, **103**, 6206.
22 D. M. Bishop, *Int. Rev. Phys. Chem.*, 1994, **13**, 21.
23 A. V. Larin and E. Cohen de Lara, *J. Chem. Phys.*, 1994, **101**, 8130.
24 A. V. Larin, F. Jousse and E. Cohen de Lara, *Stud. Surf. Sci. Catal.*, 1994, **84**, 2147.
25 A. V. Larin and E. Cohen de Lara, *Mol. Phys.*, 1996, **88**, 1399.
26 F. Jousse, A. V. Larin and E. Cohen de Lara, *J. Phys. Chem.*, 1996, **100**, 238.
27 G. Maroulis, *J. Phys. Chem.*, 1996, **100**, 13 466.
28 F. P. Billingsley and M. Krauss, *J. Chem. Phys.*, 1974, **60**, 4130.
29 G. Maroulis and A. J. Thakkar, *J. Chem. Phys.*, 1988, **88**, 7623.
30 R. D. Amos, *Mol. Phys.*, 1980, **39**, 1.
31 R. K. Nesbet, *J. Chem. Phys.*, 1964, **40**, 3619.
32 F. P. Billingsley and M. Krauss, *J. Chem. Phys.*, 1974, **60**, 2767.
33 R. D. Amos, *Chem. Phys. Lett.*, 1979, **68**, 536.
34 L. L. Poulsen, *Chem. Phys.*, 1982, **68**, 29.
35 G. H. F. Diercksen and A. J. Sadlej, *Chem. Phys.*, 1985, **96**, 17.
36 G. Maroulis, *Z. Naturforsch. A*, 1992, **47**, 480.
37 J. G. Kirkwood, *Phys. Z.*, 1932, **33**, 57.
38 A. V. Larin and D. P. Vercauteren, *J. Phys. Chem. B*, submitted for publication.
39 R. J. Le Roy, *LEVELS program*, Department of Chemistry, University of Waterloo, Waterloo, Ontario N2L 3G1, Canada, 1989.
40 A. V. Larin and V. S. Parbuzin, *Mol. Phys.*, 1992, **77**, 869.
41 G. A. Victor and A. Dalgarno, *J. Chem. Phys.*, 1970, **53**, 1316.
42 K. Ogawa, M. Nitta and K. Aomura, *J. Phys. Chem.*, 1978, **82**, 1655.
43 K. Zeff and D. P. Shoemaker, *Acta Crystallogr.*, 1967, **22**, 162.
44 J. J. Pluth and J. V. Smith, *J. Am. Chem. Soc.*, 1980, **102**, 4704.
45 E. Cohen de Lara and T. T. Nguyen, *J. Phys. Chem.*, 1976, **80**, 1917.
46 W. J. Mortier, P. Geerlings, C. Van Alsenoy and H. P. Figeys, *J. Phys. Chem.*, 1979, **83**, 855.
47 S. Beran and J. Dubský, *J. Phys. Chem.*, 1979, **83**, 2538.
48 H. Förster and W. Frede, *Infrared Phys.*, 1984, **24**, 151.
49 J. J. Camacho, A. Pardo and J. M. L. Poyato, *J. Chem. Soc., Faraday Trans.*, 1994, **90**, 23.
50 H. M. Hulburt and J. O. Hirschfelder, *J. Chem. Phys.*, 1941, **9**, 61.
51 H. Böse and H. Förster, *J. Mol. Struct.*, 1990, **218**, 393.
52 A. V. Larin, *Chem. Phys. Lett.*, 1995, **232**, 383.
53 In the erratum by A. V. Larin, *Chem. Phys. Lett.*, 1995, **238**, 208 to ref. 52, an error was made because of the incorrect expression of the cubic anharmonicity coefficient a_1. With the correct expression $a_1 = (-1 - \alpha_e\omega_e/(6B_e^2))$, the Buckingham formula leads to a BS value underestimated by a factor of 3 as compared to the experimental value for H_2 (while using the same derivatives as in ref. 23) in accordance with the correct conclusion of ref. 52.
54 J. O. Hirschfelder, C. F. Curtiss and R. B. Bird, *Molecular Theory of Gases and Liquids*, Wiley, London, 1954.
55 T. Masuda, K. Tsutsumi and H. Takahashi, *J. Colloid Interface Sci.*, 1980, **77**, 238.
56 D. Basmadjian, *Can. J. Chem.*, 1960, **38**, 141.
57 D. M. Ruthven and R. L. Derrah, *J. Chem. Soc., Faraday Trans. 1*, 1975, **71**, 2031.
58 A. V. Larin, D. P. Vercauteren, C. Lamberti, S. Bordiga and A. Zecchina, *Phys. Chem. Chem. Phys.*, 2002, **4**, DOI: b107242k.
59 A. J. Stone and M. Alderton, *Mol. Phys.*, 1985, **56**, 1047.
60 A. V. Larin, L. Leherte and D. P. Vercauteren, *Chem. Phys. Lett.*, 1998, **287**, 169.
61 A. V. Larin and D. P. Vercauteren, *Int. J. Quantum Chem.*, 1998, **70**, 993.
62 A. V. Larin and D. P. Vercauteren, *Int. J. Inorg. Mater.*, 1999, **1**, 201.
63 A. V. Larin and D. P. Vercauteren, *J. Mol. Catal. A*, 2001, **168**, 123.
64 A. V. Larin and D. P. Vercauteren, *J. Mol. Catal. A*, 2001, **166**, 73.
65 R. Dovesi, V. R. Saunders, C. Roetti, M. Causà, N. M. Harrison, R. Orlando and E. Aprà, *CRYSTAL95 1.0, User's Manual*, 1996.
66 A. V. Larin and D. P. Vercauteren, *Int. J. Quantum Chem.*, 2001, **83**, 70.